(12)

UNCLASSIFIED

RANRL-TN-3/85

AR Number 003-429

AD-A161 542

DEPARTMENT OF DEFENCE

DEFENCE SCIENCE AND TECHNOLOGY ORGANISATION

WEAPONS SYSTEMS RESEARCH LABORATORY

RAN RESEARCH LABORATORY

RANRL TECHNICAL NOTE NO. 3/85

MODELLING THE RADAR EVAPORATIVE DUCT

By

M.R. BATTAGLIA

APPROVED FOR PUBLIC RELEASE

COPY NO:

APRIL 1985

UNCLASSIFIED

JN0298
D18000

DEPARTMENT OF DEFENCE

WEAPONS SYSTEMS RESEARCH LABORATORY

RAN RESEARCH LABORATORY

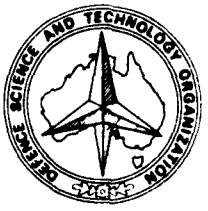

RANRL TECHNICAL NOTE NO. 3/85

MODELLING THE RADAR EVAPORATIVE DUCT

By

M.R. BATTAGLIA

ABSTRACT

A model of the radar evaporative duct is described, based on Monin-Obukov similarity theory. The similarity functions, Monin-Obukov stability length and scaling parameters are derived from experimental data. Graphs are presented for duct heights and the number of trapped modes at 10 GHz for a wide range of environmental conditions.

POSTAL ADDRESS: The Superintendent, Maritime Systems Division, RAN Research Laboratory, PO Box 706 Darlinghurst, NSW 2010

JN0298
D18000

CONTENTS

1. INTRODUCTION

A decrease in refractive index with height causes rays of electromagnetic radiation to bend towards the earth's surface. The mean rate of change of refractive index near the earth's surface determines the earth's 'effective radius' and radar horizon [1]. When the rate of change of refractive index equals a critical value, the earth's effective radius and radar horizon become infinite. This is the condition for super-refraction. Greater rates of change result in radar 'ducts', for which the field strengths for microwave propagation are not calculable by simple ray theory and require calculation by mode theory [2] or hybrid models.

The input to any such theoretical model is information about

(i) the vertical rate of change of refractive index in the atmosphere and (in the case of surface-based ducts)

(ii) the reflectivity of the rough sea surface.

Only the latter is adequately described by both theory and experimental data [1]. Surface-based ducts near land may be advective [3], but well removed from continental effects and at low altitudes the most important mechanism is surface evaporation. The refractive index variation for elevated ducts and advective ducts can be obtained from radiosonde measurements of temperature, humidity and height or pressure. In the case of surface evaporative ducts, which are only 5-25 metres in height, these variables cannot easily be measured with sufficient precision and a profile model must be used. Typically these models require as inputs only a few simple bulk environmental parameters such as air and sea temperature, relative humidity and wind speed at one height. From these, profiles of

refractive index can be deduced which are in reasonable agreement with direct measurements - especially when the air and sea temperatures are nearly equal [4-9]. This note briefly summarizes existing models and experimental data for the evaporative duct, and presents relations and algorithms which are valid over a wider range of environmental conditions.

The outputs of the model include

(i) refractivity profiles and duct height, and

(ii) the frequency-dependence of trapping expressed as either the number of trapped modes at a given frequency, or the cut-off frequency.

2. THEORY

2.1 Refractivity

The refractive index (n) at microwave frequencies is dependent mainly on water vapour pressure (e), temperature (T) and atmospheric pressure (p). The refractivity (N) is described by the Debye formula [10],

$$N = 10^6(n-1)$$

$$\approx \frac{77.6}{T}\left(p + \frac{4810\ e}{T}\right) \qquad (1)$$

with p and e in mbar and T in Kelvin. The rate of change of refractive index with height (z) is obtained by differentiating equation 1

$$\frac{dN}{dz} = \left(\frac{\partial N}{\partial p}\right)\frac{dp}{dz} + \left(\frac{\partial N}{\partial T}\right)\frac{dT}{dz} + \left(\frac{\partial N}{\partial e}\right)\frac{de}{dz} \qquad (2)$$

Evaluating (2) at sea level (p_o = 1013.25, T_o = 288.15 e_o = 10.13) for the standard atmosphere gives

$$\frac{dN}{dz} = 0.269\ \frac{dp}{dz} - 1.263\ \frac{dT}{dz} + 4.495\ \frac{de}{dz} \qquad (3)$$

The change with pressure is fairly insensitive to climatic variations, and pressure at low altitudes is well described by the barometric formula

$$p = p_o e^{-z/H_o} \qquad (4)$$

where $H_o \approx 7300$ metres. The surface duct height is defined as the height corresponding to the minimum of the modified refractivity

$$M = N + 10^6\ z/a \qquad (5)$$

where a is the earth radius. That is, the duct height corresponds to the altitude where

$$\frac{dN}{dz} = -0.157\ m^{-1} \qquad (6)$$

Combining this with equations 3 to 5 leads to the duct-height relation

$$4.495\ (de/dz) - 1.263\ (dT/dz) = -0.125 \qquad (7)$$

The solution of eq (7) is single-valued for the evaporative duct. Once the humidity and temperature profiles are known it is then a straightforward matter, not only to derive the duct height, but also to determine the M-profile which allows further analysis of the frequency-dependence of trapping in the duct [2].

2.2 Neutral Profiles

If the boundary layer adjacent to the sea surface is neutrally buoyant, which occurs when the temperature of the air and sea are approximately equal, the conditions are said to be of neutral stability. The boundary layer can be defined [5] as the layer in which the fluxes of sensible heat (H_S), latent heat (H_L) and momentum ($-\tau$) are constant (to within, say, 5%). These fluxes can be written as

$$H_S = \rho C_p \overline{t' u_3'} \tag{8}$$

$$H_L = \rho L \overline{q' u_3'} \tag{9}$$

$$\tau = -\rho \overline{u_1' u_3'} \tag{10}$$

where q', t', u_1' and u_3' are fluctuations in moisture, temperature, downwind component of wind and vertical component of wind respectively. The overbar denotes an average over sufficiently long time, say one hour, for the averages to reach a statistically stable value. From Monin-Obukov similarity theory [b] there exist a scaling temperature (T_*), scaling moisture (q_*), and friction velocity (u_*) which facilitate unique descriptions of non-dimensional vertical profiles (T/T_*), (q/q_*) and (U/u_*) for given stability conditions. The fluxes can then be parameterized as

$$H_L = \alpha K \rho L u_* q_* \tag{11}$$

$$H_S = \alpha K \rho C_p u_* T_* \tag{12}$$

$$\tau = -\rho u_*^2 \tag{13}$$

where K is von Karman's constant, ρ is the density of air, C_p is the heat capacity of air, and L is the latent heat of vaporization. The constant α is the ratio of the eddy diffusivities of heat and momentum which is usually assumed to be unity [5] but has been shown from experiment to be around 1.35 [11]. This uncertainty will not affect the conclusions in this section since we define the scaling parameters according to the gradients under neutral conditions

$$\frac{dU}{dz} = \frac{u_*}{Kz} \tag{14}$$

$$\frac{dT}{dz} = \frac{T_*}{Kz} \tag{15}$$

$$\frac{dq}{dz} = \frac{q_*}{Kz} \tag{16}$$

Integration of (14) - (16) leads to the mean quantities

$$U = \frac{u_*}{K} \ell n(z/z_0) \tag{17}$$

$$T = T_0 + \frac{T_*}{K} \ell n(z/z_0) \tag{18}$$

$$q = q_0 + \frac{T_*}{K} \ell n(z/z_0) \tag{19}$$

where T_0 is the temperature and q_0 is the mixing ratio at $z=z_0$. The latter is the roughness length for momentum which has been experimentally related to the friction velocity [12]

$$z_0 = a\, u_*/g + (\nu/u_*)\, e^{-5.5K} \tag{20}$$

where a is the Charnock-Ellison constant (≈ 0.011), $g = 9.8$ m/sec^2 and ν is the kinematic viscosity of air ($\nu \approx 14 \times 10^{-6}$ m^2/sec). The first term in eq (20) represents the increase in surface roughness with

increasing wind stress owing to surface waves, while the second term represents an aerodynamically smooth surface and is important for wind speeds less than a few metres per second. Typical values for moderate wind (U_{10} = 10m/sec) are $u_\star$ = 0.36 m/sec and $z_0 = 1.5 \times 10^{-4}$ m. In some models of the evaporative duct [6,7] z_0 is taken as a constant roughness length with a value of $\sim 1.5 \times 10^{-4}$m. This assumption is probably adequate as

(i) we are not concerned with the behaviour at heights which are less than the wavelength of microwave radiation, and

(ii) the integration constants T_0 and q_0 are probably not measurably different from the bounds determined by the sea surface temperature.

The scaling factors for neutral profiles can then be determined from the expressions

$$u_\star = \frac{KU_1}{\ln(z_1/z_0)} \tag{21}$$

$$T_\star \simeq \frac{u_\star (T_1 - T_0)}{U_1} \tag{22}$$

$$q_\star \simeq \frac{u_\star(q_1 - q_0)}{U_1} \tag{23}$$

where T_1, U_1, q_1 are the temperature, wind speed and humidity measured at $z = z_1$. For moderate winds $u_\star/U \simeq 0.038$ m/sec [4,8] so that, when $T_1 \simeq T_0$ the above relations reduce, after some substitution, to a simple expression for the duct height in terms of 10-metre bulk differences

$$d \simeq 0.96\,(T_{10} - T_0) - 3.4\,(e_{10} - e_0) \qquad (24)$$

with e in mbar and T in Kelvin. For typical moisture gradients of up to 10 mbar in 10 metres, neutral duct heights are up to 30 metres, with the temperature term being of little importance.

The assumption of a constant drag coefficient (u_*^2/U^2) for a given measurement height, and a simple relation between wind and humidity profiles, leads to the conclusion that neutral duct heights are independent of wind speed for given humidity difference. This is a common feature of most of the models in the literature for neutral duct heights [4, 6-8]. If the magnitude of the air-sea temperature difference is significant, the above models are not adequate and the effect of stability must be taken into account.

2.3 Stable and Unstable Profiles

When the air is warmer than the sea the conditions are said to be stable, and a warmer sea is said to be unstable. According to Monin-Obukov similarity theory, the gradients at height z in the boundary layer can be determined from T_*, q_*, u_* and a dimensionless height (z/L). The calculation of the Monin-Obukov stability length (L) will be outlined in section 2.5.

The gradients of U, T and q can be written in terms of stability functions $\phi(z/L)$

$$\frac{dU}{dz} = \frac{u_*}{Kz} \phi_u(z/L) \tag{25}$$

$$\frac{dT}{dz} = \frac{T_*}{Kz} \phi_T(z/L) \tag{26}$$

$$\frac{dq}{dz} = \frac{q_*}{Kz} \phi_q(z/L) \tag{27}$$

Universal profiles $\Psi_i\ (z/L)$ are related to $\phi_i(z/L)$ [5] as

$$\Psi_i\ (z/L) = \int_{z_0/L}^{z/L} \frac{1 - \phi_i(z/L)}{z/L}\ d(z/L) \tag{28}$$

or

$$\Phi_i(z/L) = 1 - z\ (d\psi_i/dz\ ) \tag{29}$$

This leads to expressions for mean quantities analogous to eqns (17) - (19),

$$U = \frac{u_*}{K} [\ \ell n\ (z/z_0) - \Psi_u\ (z/L)\ ] \tag{30}$$

$$T = T_0 + \frac{T_*}{K} [\ \ell n\ (z/z_0) - \Psi_T\ (z/L)\ ] \tag{31}$$

$$q = q_0 + \frac{q_*}{K} [\ \ell n\ (z/z_0) - \Psi_q\ (z/L)\ ] \tag{32}$$

It follows from (28) that T_0 and q_0 are defined as the values of T and q evaluated at $z=z_0$ (the roughness length for momentum). The error in equating these to the equilibrium sea-level values should be negligible. A more detailed discussion is given in Annex A.

2.4 Empirical Stability Functions

All profiles have the feature that as $z/L \to 0$, $\phi_i \to 1$ and $\Psi_i \to 0$. Under stable conditions, the stability functions can be approximated by the first two terms in the Taylor series expansion

$$\phi_i \approx 1 + \alpha_i (z/L) \qquad z/L > 0 \qquad (33)$$

where $\alpha_u = 4.5$ [7] and $\alpha_T = \alpha_q = 6.35$ [11].

Under unstable conditions the stability functions are very non-linear in z/L. Under these conditions the stability function for wind follows the Keyps profile [5] which can be approximated as [11]

$$\phi_u \approx (1 - 18\,(z/L))^{-1/4} \qquad z/L < 0 \qquad (34)$$

Temperature and humidity functions for unstable conditons are in good agreement with the expression [11]

$$\phi_T = \phi_q = (1 - 9\,(z/L))^{-1/2} \qquad z/L < 0 \qquad (35)$$

From equation (28) the universal profiles follow as

$$\Psi_u = -4.5\,(z/L) \qquad z/L > 0 \qquad (36)$$

$$\Psi_T = \Psi_q = -6.35(z/L) \qquad z/L > 0 \qquad (37)$$

$$\Psi_T = \Psi_q = \ell n \left[\frac{\sqrt{1-9\,z/L}+1}{\sqrt{1-9\,z/L}-1} \cdot \frac{\sqrt{1-9\,z_o/L}-1}{\sqrt{1-9\,z_o/L}+1} \cdot \frac{z}{z_o} \right] \qquad z/L < 0 \qquad (38)$$

The function $\Psi_u\,(z/L)$ for unstable conditions is calculated from a fit of the numerical integration [5, 7] of ϕ_u.

2.5 Monin - Obukov Stability Length

The dimensionless quantity (z/L) is the ratio of convective to mechanical energy production in near neutral air [5]. The Monin-Obukov stability length (L) can then be written as

$$L = \frac{u_*^3 \, T}{K \, g \, (\overline{t' u_3'} + 0.608 \, T \, \overline{q' u_3'})} \tag{39}$$

The sensible heat flux ($\rho \, C_p \, \overline{t' u_3'}$) and moisture flux ($\rho \, \overline{q' u_3'}$) are not easily measured, and various parameterization schemes have been proposed. Most are of the form [13]

$$\overline{u_3' t'} = A + B \, U_z \, \Delta T \tag{40}$$

$$\overline{u_3' q'} = C_E \, U_z \, \Delta q \tag{41}$$

where U_z is the mean wind speed at the reference height, and ΔT and Δq are the air-sea temperature and moisture differences respectively. These will not be used in this model for reasons of internal consistency, but are useful for parametric schemes of evaporative duct height in near-neutral conditions [4].

A quantity which is closely related to z/L is the gradient Richardson number Ri.

$$Ri = \frac{g \, (\partial T / \partial z)}{T \, (\partial U / \partial z)^2} \tag{42}$$

From the profile relations in the previous sections, (42) can be re-written as

$$Ri = \frac{gz\Delta T}{T\,U^2} \cdot \left(\frac{(\ell n\,(z_1/z_0) - \Psi_u)^2}{(\ell n\,(z_1/z_0) - \Psi_T)} \cdot \frac{\phi_T\,(z/L)}{\phi_u^2\,(z/L)} \right) \qquad (43)$$

For near-neutral conditions, with U and T measured at 6 metres, the term in brackets is of order 10. Under these conditions, (43) reduces to the definition of the bulk Richardson number used in refs [6] and [7]

$$R_{ib} = \frac{10\,gz\Delta T}{T\,U^2} \qquad (44)$$

In ref.[7], R_{ib} is first calculated according to eqn (44) and z/L is then calculated by a simple empirical fit.

In this model we prefer to use eqn 39 directly, with terms in $\overline{t'u_3'}$ and $\overline{q'u_3'}$ replaced by terms in scaling temperatures and moisture respectively

$$L = \frac{u_*^2\,T}{1.35\,K\,g\,(T_* + 0.608\,T\,q_*)} \qquad (45)$$

where the factor 1.35 arises because T_* and q_* are defined here in terms of the respective gradients and not the fluxes. Businger [11] has measured this quantity which is a ratio of eddy diffusivities, by comparing the two methods of calculation from flux and profile measurements. The difficulty with (45) is that U_*, T_* and q_* are themselves functions of L

$$u_* = KU_1 / \left(\ell n\,(z_1/z_0) - \Psi_u\,(z_1/L) \right) \qquad (46)$$

$$T_* = K\,(T_1 - T_0) \,/\, \left[\ell n\,(z_1/z_0) - \Psi_T\,(z_1/L) \right] \qquad (47)$$

$$q_* = K\,(q_1 - q_0) \,/\, \left[\ell n\,(z_1/z_0) - \Psi_q\,(z_1/L) \right] \qquad (48)$$

The model solves (45) - (48), which are well-behaved functions, by a stepwise refinement iterative procedure. Given a reasonable first guess for L, the test quantity 1/L converges to 10^{-4} metre typically in 3-4 iterations.

Comparisons of R_{ib}, z_1/L (ref.7) and z_1/L (iterative solution) are shown in figure 1. The bulk Richardson number as defined in (42) is not a particularly good estimator, since the density gradients are approximated by temperature gradients, and does not account for the fact that moist air is less dense than dry air. According to similarity theory the Richardson number is a unique function of L and so figure 1 could be used as a look-up graph. However, in order to compare L from either a parametric model (eqns 39-41) or equation 45, the Richardson numbers need to be defined in terms of virtual temperature (T_v)

$$T_v \simeq T\,(\,1 + 0.608\,q\,) \qquad (49)$$

and

$$\Delta T_v \simeq \Delta T + 0.107\,\Delta e \qquad (49(a))$$

in which q is the mixing ratio and Δe is the change in water vapour pressure in mbar. Typical Δe for tropical waters is -10 mbar [4], so that neutral conditions occur at $\Delta T \approx +1$ deg. Celsius.

From figure 1 it is clear that, over a moderate range of temperatures (and therefore saturated vapour pressures) and relative humidities, z_1/L calculated by the method of ref. 7 is not sufficiently accurate for the model described here. It is used, however, as a first guess for the iterative algorithm for L, except for weakly unstable conditions where it predicts the wrong sign for L.

2.6 Calculation of the Evaporative Duct Height

The evaporative duct height is defined as the height at which the modified refractivity (M) is a minimum. From eq (7),

$$-0.125 = 4.495\ c \left(\frac{dq}{dz}\right) - 1.263 \left(\frac{dT}{dz}\right) \tag{50}$$

where c is the ratio of water vapour pressure in mbar to mixing ratio (≈ 1630). It is convenient here to define a new variable N′, closely related to the refractivity, for which the rate of change of N′ with height is the rate of change of N less that due to pressure alone;

$$\frac{dN'}{dz} = 4.495\ c \left(\frac{dq}{dz}\right) - 1.263 \left(\frac{dT}{dz}\right) \tag{51}$$

$$= 4.495\ c\ \frac{q_\star}{Kz}\ \phi_q(z/L) - \frac{1.263\ T_\star}{Kz}\ \phi_T(z/L) \tag{52}$$

Now if $\phi_T \approx \phi_q$, N′ follows the similarity rules

$$\frac{dN'}{dz} = \frac{N_\star}{Kz}\ \phi_N(z/L) \tag{53}$$

where $\phi_N \approx \phi T \approx \phi_q$ and

$$N_\star = 4.495\ c\ q_\star - 1.263\ T_\star \tag{54}$$

The duct-height (z) is then obtained from the relation

$$N_* \; \phi_N(z/L) \quad = \quad -0.125 \; K \; z \qquad (55)$$

In the program, equation (55) is solved by the secant iterative method, and z usually converges to with 10^{-3} metre after 2 iterations.

Results for two extremes of relative humidity (30% and 90%) are shown in figures 2-6 for Ts = 15, 18, 21, 24 and 28 degrees Celsius. In all cases duct height increases with wind speed in the unstable region (Ta - Ts < 0) and is wind-speed-independent for neutral conditions. The effect is reversed for stable conditions.

Results for the lowest wind speed (3 m/sec) are not plotted past $\Delta T \simeq 0.5°C$ since this corresponds to z/L > 0.1, which is the limit of validity of this model and of similar models based on turbulence theory [5]. The lower limit (z/L ≃ -1) seems a less important bound since the scaling laws extrapolate adequately in the unstable region [8].

2.7 Comparison with other Models

Most models of the surface evaporative duct, which can be found in the literature, provide similar results for neutral conditions. This is because the neutral drag coefficient is independent of wind speed, so that the duct height is approximately linear in the humidity difference. The results of Jones and Stewart [4] reduce, after some substitution to

$$d \quad = \quad 2.50 \; (e_0 - e_{10}) \qquad (56)$$

where e_{10} is the water vapour pressure in mbar at 10 metres, and e_0 is the sea level value. The difference in the numerical factor between this result and equation (24) is due to different values used for the friction velocity and heat transfer coefficients. The Hitney model [7] (also used in the NOSC 'IREPS' computer program) covers unstable, neutral and stable conditions and reduces to a closed form expression

$$d = \frac{\Delta N}{b_1 \left(\ell n(z_1/z_0) + 5.2\, z_1/L \right) - 5.2\, \Delta N/L} \qquad (57)$$

for stable conditions and an analogous expression for unstable conditions. Although no derivation is given, the model is similar to that used by Jeske [6] which assumes identical stability functions for wind, temperature and moisture. It also appears to assume that $\partial N/\partial z$ is linear combination of Δe and ΔT. Under neutral conditions the Hitney/Jeske models reduce to

$$d = 0.025 + 3.4\ (e_0 - e_{10}) \qquad (58)$$

which is very close to the result of the model (eq 24). For stable and unstable conditions, the general trends with temperature difference and wind speed are similar, the main difference being due to the use of normalized wind profiles for temperature and moisture.

The USN Weather Service model [8] is closer to that described here except that, in order to avoid iterative solutions, the equality of wind, temperature and moisture stability functions was also assumed. The USN model reduces to the general expressions

$$d = \phi_u\ (z_1/L)\ (A\, q_\star - B\, T_\star) \qquad (59)$$

where A and B are constants determined by the selected reference level (z_1).

2.8 Frequency-dependence of Duct Strength

The ability of a duct to support trapped modes increases with duct height, frequency and ΔM [2]. In order to calculate the signal strength in the duct it is necessary to use mode theory [2,9], but this is not feasible for routine environmental predictions.

The phase criteria for trapped rays can be readily calculated from ray theory by considering the ray to be composed of two components - one ray propagating along the duct axis, and a standing wave in the vertical direction. The condition for maximum energy flow along the duct requires that 'similar points' for a ray be in phase, and this is calculable by considering only the vertical ray and two reflections - one at the sea surface and the other at some turning point, b_m [2]. The grazing angle for the surface reflection is sufficiently small for the phase change on reflection to be equated to 180°, and so the phase condition is

$$\frac{2\sqrt{2}\times 10^{-3}}{\lambda}\int_0^{b_m}\sqrt{M(z)-M(d)}\,dz = m - 1/4,\quad m = 1,2,3.. \qquad (60)$$

where d is the duct height. When b_m is set to d, the solution of (60) yields the number of trapped modes (m). When m=1, the solution gives the maximum trapped wavelength λ or minimum trapped frequency, or cut-off frequency, (f_{co}).

In general, equation (60) cannot be solved analytically and the M-profile must be broken up into integrable segments. In the model n = 100 linear segments are used, but n as low as 10 may give adequate results for most purposes as long as the M-profile is well described in the lowest 10 or so metres, where most of the M-deficit occurs.

In each linear segment a slope (k_i) and intercept (M_{oi}) are defined so that, in the ith segment,

$$M_i(z) = M_{oi} - k_i z \tag{61}$$

and equation (60) can be rewritten as

$$m - 1/4 = \frac{2\sqrt{2} \times 10^{-3}}{\lambda} \sum_{i=o}^{n-1} \int_{id/n}^{(i+1)d/n} \sqrt{k_i (d-z)}\, dz$$

$$= \frac{2\sqrt{2} \times 10^{-3}}{\lambda} \sum_{i=o}^{n-1} -\frac{2}{3} k_i^{1/2} d^{3/2} \left[\left(1 - \frac{i+1}{n}\right)^{3/2} - \left(1 - \frac{i}{n}\right)^{3/2} \right] \tag{62}$$

where

$$k_i = n(M_{i+1} - M_i) / d \tag{63}$$

for equal sized segments.

Setting m = 1 and solving for frequency (c/λ) yields the nominal cut-off frequency (f_{co}), which is one of the outputs of the program. The number of trapped modes at any other frequency (f) is then simply

$$m = 0.25 + 0.75\,(f/f_{co}) \tag{64}$$

Equation (64) allows non-integer values of m. In ray theory the turning point is well-defined for any ray so that only the integer part of m is significant. (That is, $m < 1$ implies no trapping). The interpretation from mode theory is that m is in the order of the number of trapped modes that need to be calculated for the contribution from trapped modes to approach convergence.

The calculated modified refractivity profiles, M(z), for several air-sea temperature differences are plotted in figure 7. The dashed line

is the "typical" refractivity profile cited in reference [2] which facilitates a rough estimate of cut-off frequency based only on the duct height and m = 1. Inspection of equation (60) and figure 7 suggests that this typical profile may over-estimate or under-estimate the cut-off frequency depending on stability. In the case of super-refraction (M fairly constant) the results would be spurious.

The general shape of the profiles in figure 7 also suggests that:

a. experimental measurement of duct height would normally be highly inaccurate since, by definition, $\partial M/\partial z = 0$ at the duct height, and

b. with equation (60) it indicates that significant variations in the limit of integration (the estimated duct height) may have little effect on the computed value of m, as long as M is well described in the lowest 10 or so metres.

The effect of stability on the number of trapped modes at 10 GHz is shown in figures 8-12. The trends are similar to those of the duct height - namely that the number of trapped modes increases with wind strength when the sea is warmer than the air and vice versa. Figs 8-12 also indicate that when the humidity is high, only one or two modes will be trapped at 10 GHz. This conclusion, as well as the dependence of duct strength on stability, was observed in very early measurements of the evaporative duct [14,15].

2.9 Propagation Modelling

Other outputs of the program include the M-profile between sea level and 100 metres, in 1-metre segments. This output, together with standard models for the rest of the troposphere [1], is the required input into microwave propagation models whether based on mode theory, ray theory or a hybrid approach [2,9].

The simplest description of the distribution of electromagnetic energy with range and height is the ray trace. Figure 13 was obtained by piping the output of the evaporative duct program into a simple ray tracing program. Work is in progress to incorporate the evaporative duct model into multipath propagation programs [1,17] to produce vertical coverage diagrams under ducting conditions.

3. SUMMARY

3.1 The model described in this note calculates duct height and an estimate of the number of trapped modes, for the surface evaporative duct under unstable, neutral and slightly stable conditions.

3.2 The empirical inputs into the model are temperature and humidity stability functions. Refractivity profiles are uniquely determined by these inputs but have not been directly measured with sufficient precision over a range of stabilities to compare with the output of the model.

3.3 No account is made of the behaviour at high wind speeds, where the effects of spray and breaking wave phenomena [16] may need to be incorporated.

3.4 In the case of neutral stability, the model gives similar results to other models in the literature. For stable and unstable conditions, no simple analytical expressions exist for the duct parameters, and iterative or recursive algorithms must be used. Representative calculations show that the convergence of the algorithms used in the model is very rapid.

3.5 The output of the associated computer program includes the modified refractivity profile, which is the required input for microwave propagation models.

REFERENCES

1. Battaglia, M.R. and Williams. P (1983). A Model of Radar Propagation and Detection. RANRL Tech Note (Ext) 2/83. UNCLASSIFIED.

2. Kerr D.E. (Ed) (1951) Propagation of Short Radio Waves. MIT Radiation Laboratory Series. Vol 13. McGraw-Hill, New York.

3. Mulhearn, P. (1978). On Surface-Based Advective Radar Ducts. RANRL Tech Note 5/78. UNCLASSIFIED.

4. Jones, I.S.F. and Stewart, R.J.J. (1977). Radar Surface Ducting in Tropical Waters. RANRL Tech Memo (Ext) 11/76. UNCLASSIFIED.

5. Lumley, J.L. and Panofsky, H.A. (1964). The Structure of Atmospheric Turbulence, Interscience, New York

6. Jeske, H. (1973). "State and Limits of Prediction Methods of Radar Wave Propagation Conditions over Sea" in Modern Topics in Microwave Propagation and Air-Sea Interaction (Ed. A. Zancla). NATO-ASI.

7. Hitney, H.V. (1975). Propagation Modelling in the Evaporation Duct. NELC Tech Report 1947.

8. NAVAIR 50-1G-522 (1975) US Naval Weather Service Numerical Environmental Products Manual. UNCLASSIFIED

9. Rotheram, S. (1973) "Modern Topics in Microwave Propagation and Air-Sea Interaction", NATO-ASI, p164.

10. Battaglia, M.R. (1979) in "Non-linear Behaviour of Atoms, Molecules and Ions in Electric, Magnetic and Electromagnetic Fields", Elsevier, Amsterdam, p 237.

11. Businger, J.A., Wyngaard, J.C., Izumi, Y and Bradley, E.F. (1971). Flux-Profile Relationships in the Atmospheric Surface Layer. J.Atmos.Sci. 28, p 181.

12. Smith, S.D. (1980) Wind Stress and Heat Flux over the Ocean in Gale Force Winds. J.Phys.Ocean. 10, p 709.

13. Friehe, C.A. and Schmitt, K.F. (1976) Parameterization of Air-sea Interface Fluxes of Sensible Heat and Moisture by the Bulk Aerodynamic Formulas. J.Phys.Ocean. 6, p 801.

14. McPetrie, J.S. and Starnecki, B. (1948) Low Level Atmospheric Ducts. Nature, 162, p 818.

15. Katzin, M., Bauchman, R.W. and Binnian W., (1947) Proc.I.R.E., 1947, p 891

16. Banner, M.L. and Melville, W.K. (1976) On the Separation of Air Flow over Water Waves. J. Fluid. Mech. 77, pp 825-842.

17. Battaglia, M.R. (1984). The Calculation of the Radar Vertical Coverage Diagram. RANRL Tech Note 1/84. UNCLASSIFED.

18. Brutsaert, W. (1975). The Roughness Length of Water Vapour, Sensible Heat and other Scalers. J.Atmos.Sci. 32, p 2028.

19. Antonia, R.A., Chambers, A.J., Rajagopalan, S., Sreenivasan, K.R. and Friehe, C.A. (1978). Measurement of Turbulent Fluxes in Bass Strait. J.Phys. Ocean. 8, p 28.

ROUGHNESS LENGTH FOR MOMENTUM, WATER VAPOUR AND SENSIBLE HEAT

If measurements of wind, humidity and temperature are made at two heights, the friction velocity (u_*), scaling moisture (q_*) and scaling temperature (T_*) can be obtained from the expressions

$$u_* = \frac{K\ (U_2 - U_1)}{\ell n(z_2/z_1) - \Psi_u(z_2/L) + \Psi_u(z_1/L)} \qquad \text{(A-1)}$$

$$q_* = \frac{K\ (q_2 - q_1)}{\ell n(z_2/z_1) - \Psi_q(z_2/L) + \Psi_q(z_1/L)} \qquad \text{(A-2)}$$

$$T_* = \frac{K\ (T_2 - T_1)}{\ell n(z_2/z_1) - \Psi_T(z_2/L) + \Psi_T(z_1/L)} \qquad \text{(A-3)}$$

where the functions $\Psi_i(z/L)$ are obtained empirically as described in section 2.4. Routine measurements at sea are made at only one height, usually around 10 metres above sea level. The second reference level is often the roughness length, or an estimate of it. The roughness length for momentum (z_0) is the height at which the wind extrapolates (using eqns 30 and 36) to zero. Similarly the roughness length for sensible heat (z_T) is the height at which the temperature extrapolates to the sea surface temperature (T_0), and the roughness length for water vapour (z_q) is the height at which the absolute humidity corresponds to the saturated humidity above sea water (q_0). It is a common feature of several models of the

evaporative duct to assume that $z_T = z_q = z_o$, and it is also assumed in some models that z_o has a constant value of 1.5×10^{-4} m [6,7]. From eqn (20), z_o increases linearly with wind speed for moderate wind speeds, so that the latter assumption is not valid. The roughness lengths for water vapour and sensible heat may also differ significantly from z_o since momemtum is transferred across the air-sea interface by both molecular diffusion and pressure forces, while heat and mass transfer are essentially controlled by molecular diffusion alone. For moderate wind speeds z_o is generally greater than z_T and z_q since, in the case of momentum, the roughness elements generate drag due to pressure forces, whereas in the case of admixture, these same elements cause a sheltering effect, inhibiting transfer at the surface [18].

The ratio of z_T and z_q to z_o can be calculated from the expressions [18]

$$z_q/z_o = 7.4 \exp(-7.3 K Sc^{1/2} R_*^{1/4}) \qquad (A-4)$$

$$z_T/z_o = 7.4 \exp(-7.3 K Pr^{1/2} R_*^{1/4}) \qquad (A-5)$$

where Sc is the Schmidt number, or ratio of kinematic viscosity of air (ν) to molecular diffusivity of water in air (≈ 0.595),
Pr is the analogous Prandtl number (≈ 0.71) for heat diffusivity,
K is von Karman's constant (≈ 0.4), and R_o is the roughness Reynolds number

$$R_o = z_o u_* / \nu \qquad (A-6)$$

Comparing eqs (A-6) and (20), R_o reduces for moderate wind speed to

ANNEX A

$$R_o \simeq 80.2\ u_*^2 \qquad (A\text{-}7)$$

with u_* in m/sec so that

$$z_T/z_o \simeq 7.4 \exp(-7.4\ u_*^{1/2}) \qquad (A\text{-}8)$$

and

$$z_q/z_o \simeq 7.4 \exp(-6.7\ u_*^{1/2}) \qquad (A\text{-}9)$$

For a moderate wind speed of U_{10} = 10m/sec (u_* = 0.38 m/sec), z_T/z_o = 0.079 and z_q/z_o = 0.116. For near-neutral conditions, the error in evaluating the scaling temperature and moisture (T_*, q_*) from eqns (18) and (19) is then approximately 20% in both cases.

Under near-neutral conditions, the evaluation of T and q at some height (z_2) other than the measurement height (z_1) can be obtained from eqns (A-2) and (A-3) with $\Psi(z/L) = 0$, without explicity calculating T_* and q_*

$$T_2 = T_o + \frac{(T_1 - T_o)\ \ell n\ (z_2/z_T)}{\ell n\ (z_1/z_T)} \qquad (A\text{-}10)$$

$$q_2 = q_o + \frac{(q_1 - q_o)\ \ell n\ (z_2/z_q)}{\ell n\ (z_1/z_q)} \qquad (A\text{-}11)$$

An order-of-magnitude error in z_T and z_q would therefore propagate an error of only a few percent of the corresponding air-sea difference for heights of 1 to 100 metres when the reference height is 10 metres.

Similar conclusions apply for non-neutral stability where differences between model predictions are more likely to be dominated by differences in stability functions $\phi(z/L)$ and $\Psi(z/L)$. It is not clear, however, that the stability functions derived from flux profile measurements are themselves not biased by the choice of z_T [11].

There is generally a paucity of experimental data for simultaneous moisture, heat and momentum flux measurements [19], which are required for the separation of the variables described in this Annex. Estimates of similarity functions, roughness lengths, scaling temperature and moisture, and von Karman's constant from limited or independent experiments are all susceptible to the type of error described above.

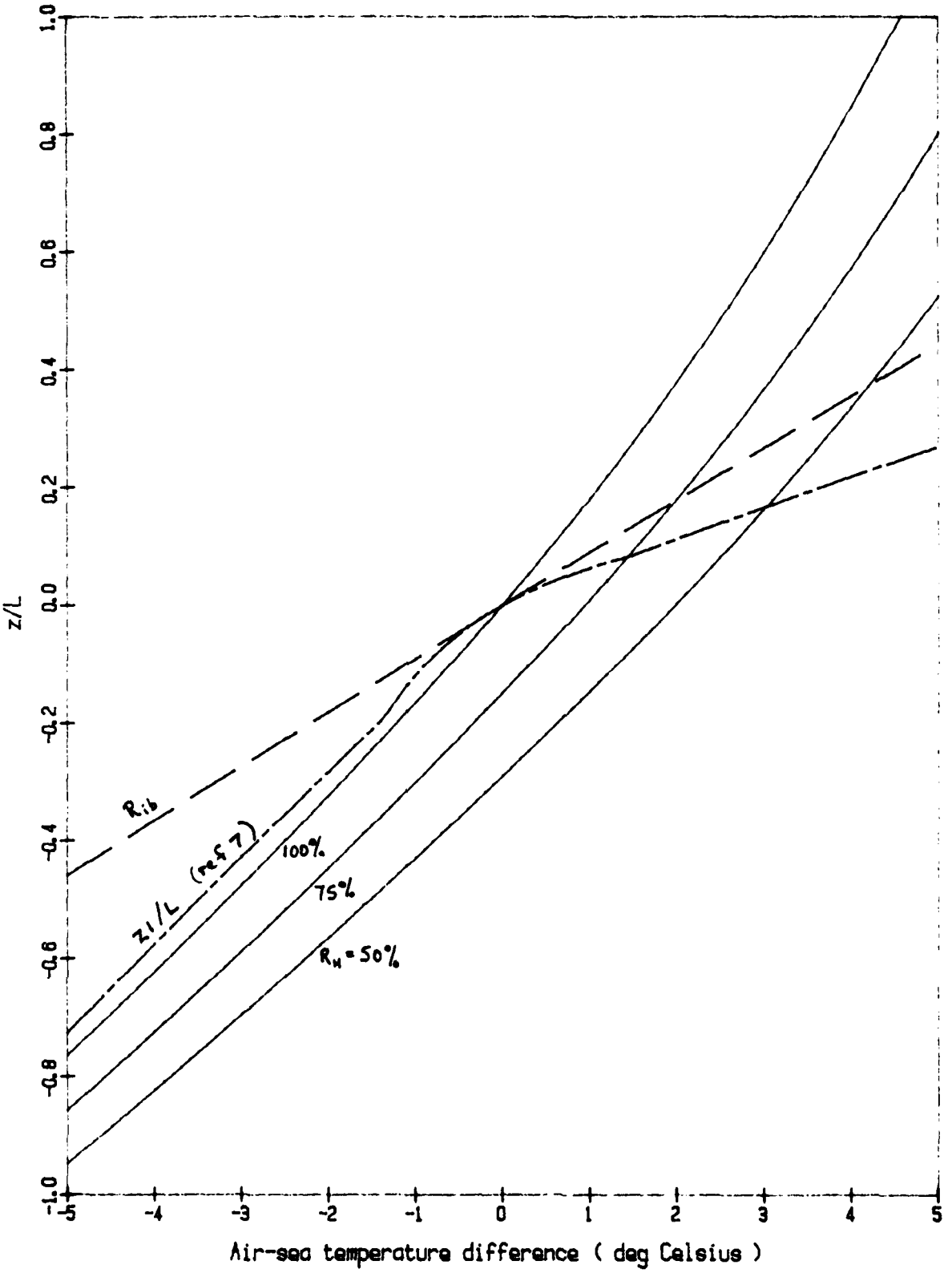

Figure 1. Comparison of z/L and two bulk estimators.
Sea temperature : 28 degrees Celsius
Wind speed : 6 m/sec
Relative humidity : 50% , 75% and 100%
Measurement height : 10 metres

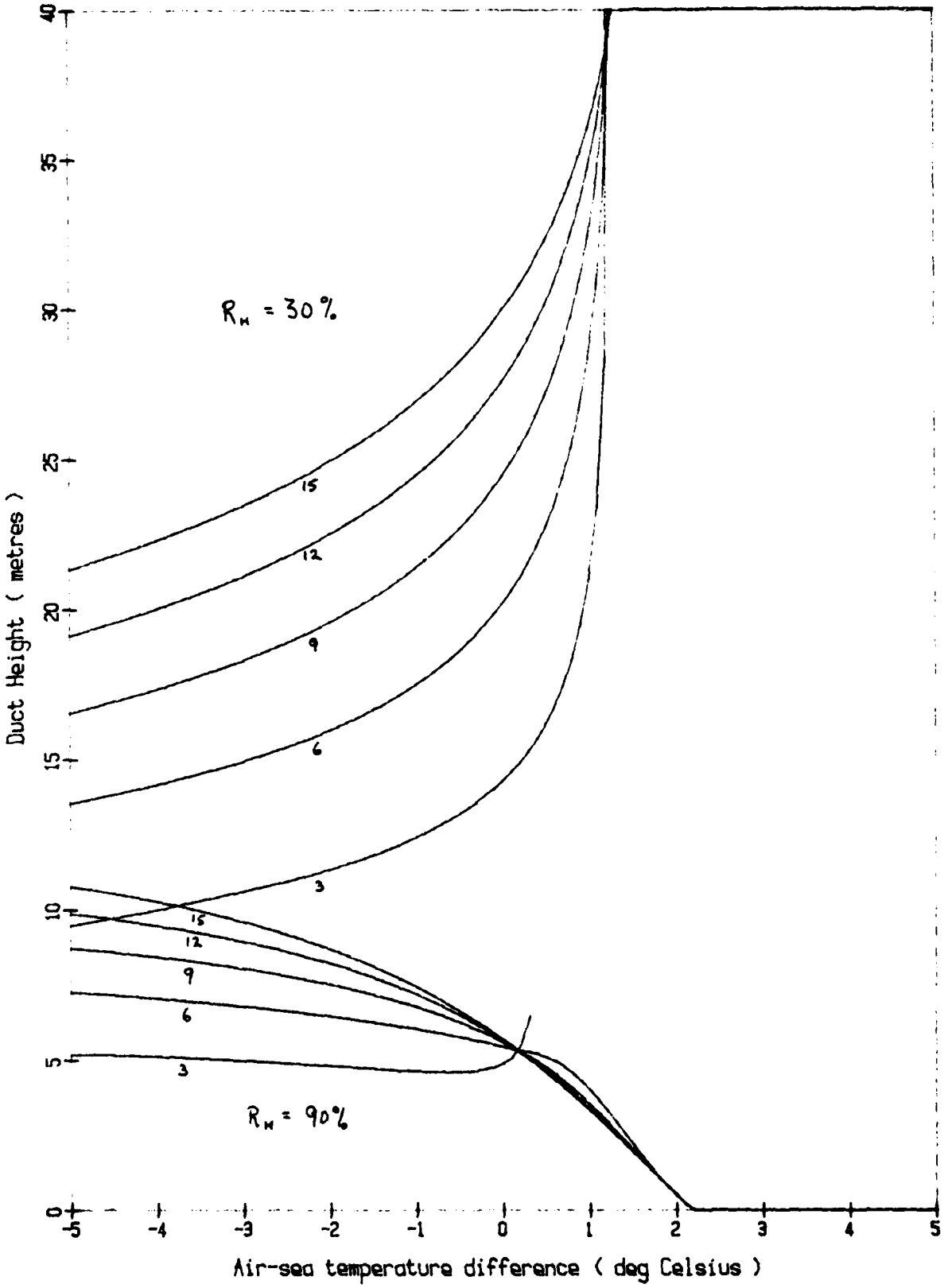

Figure 2. Calculated evaporative duct height for sea temperature of 15 deg C.
Wind speed : 3, 6, 9, 12, and 15 m/sec
Relative humidity : 30% and 90%
Measurement height : 10 metres

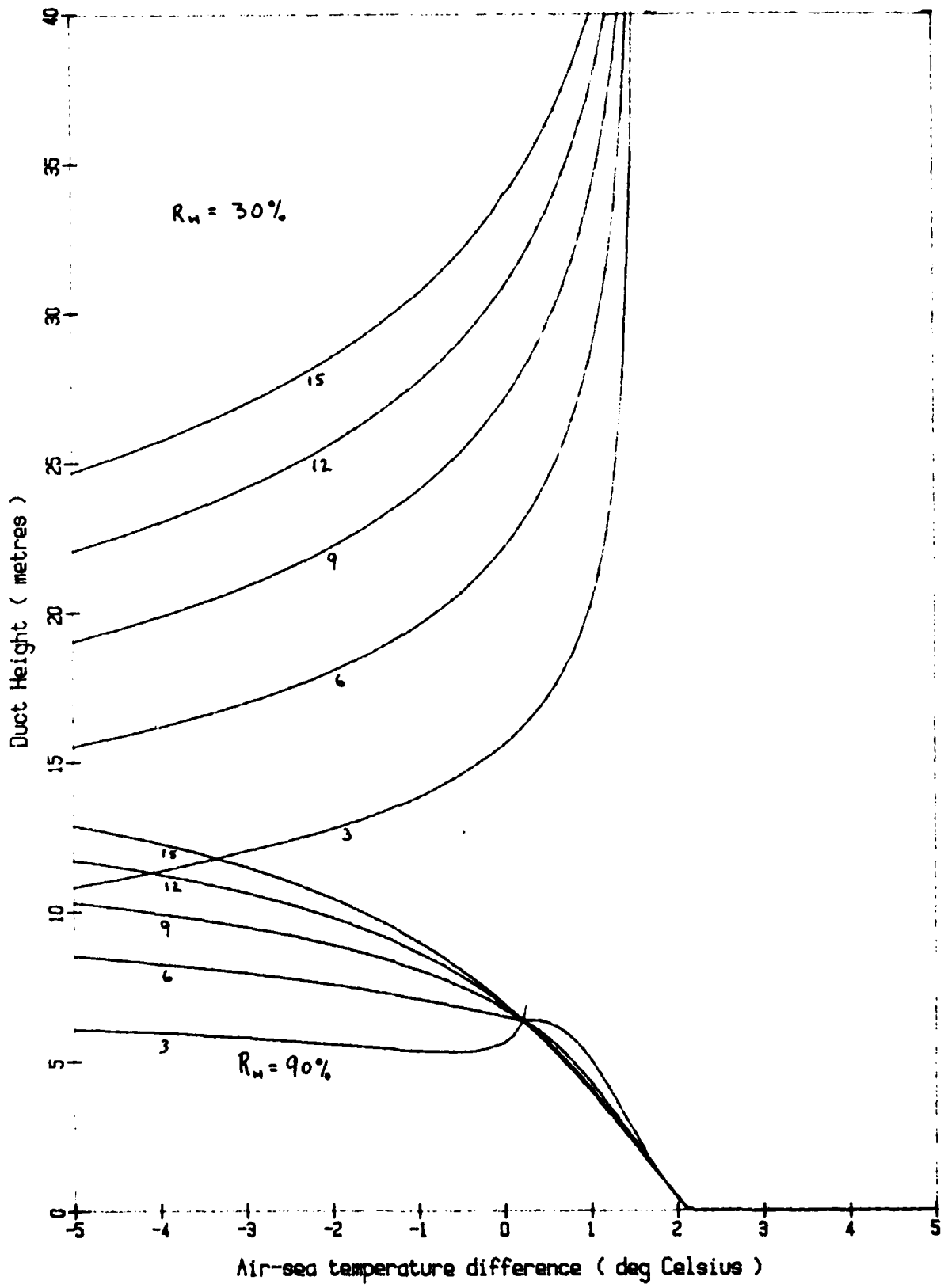

Figure 3. Calculated evaporative duct height for sea temperature of 18 deg C.
Wind speed : 3, 6, 9, 12, and 15 m/sec
Relative humidity : 30% and 90%
Measurement height : 10 metres

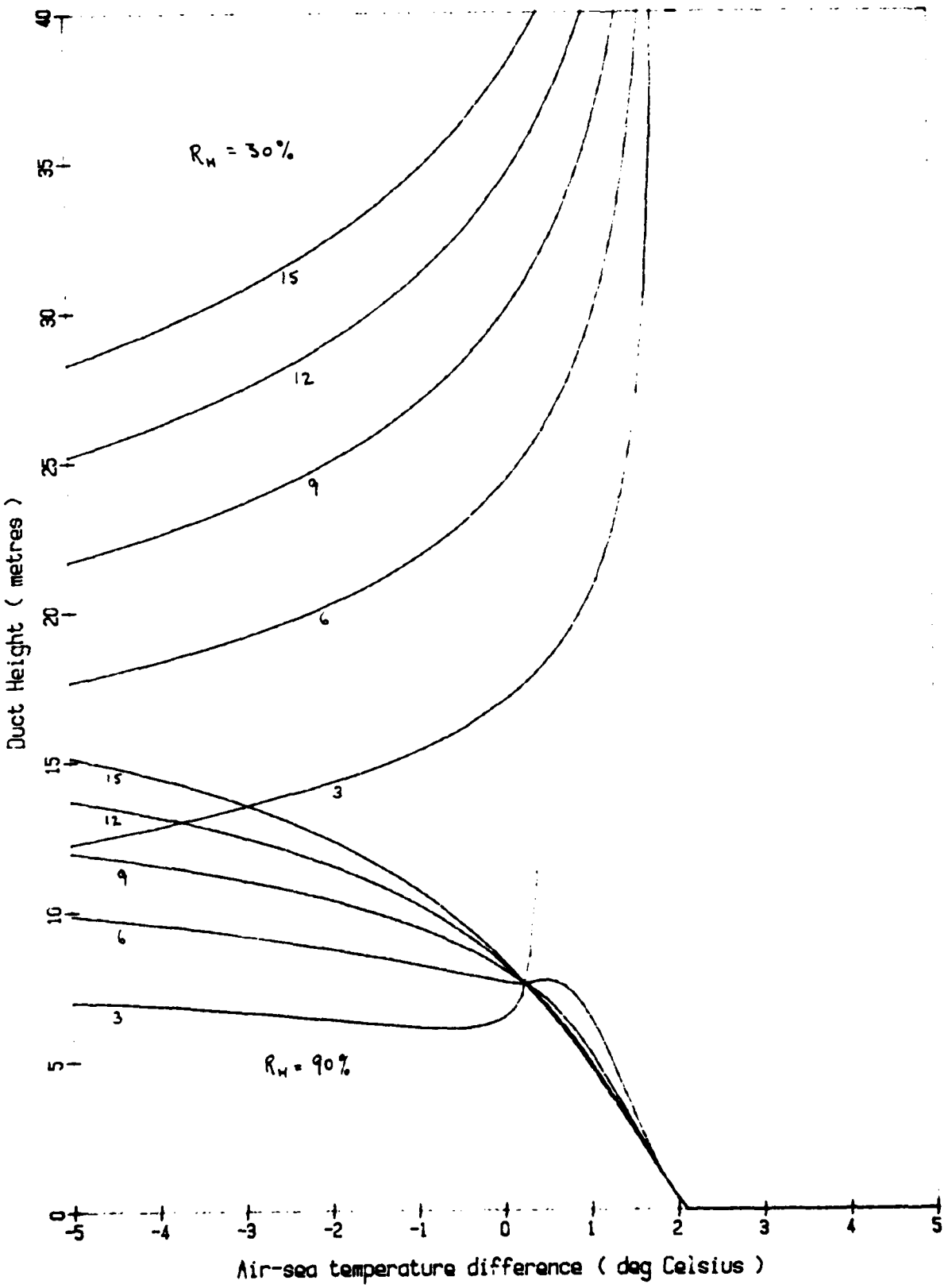

Figure 4. Calculated evaporative duct height for sea temperature of 21 deg C.
Wind speed : 3, 6, 9, 12, and 15 m/sec
Relative humidity : 30% and 90%
Measurement height : 10 metres

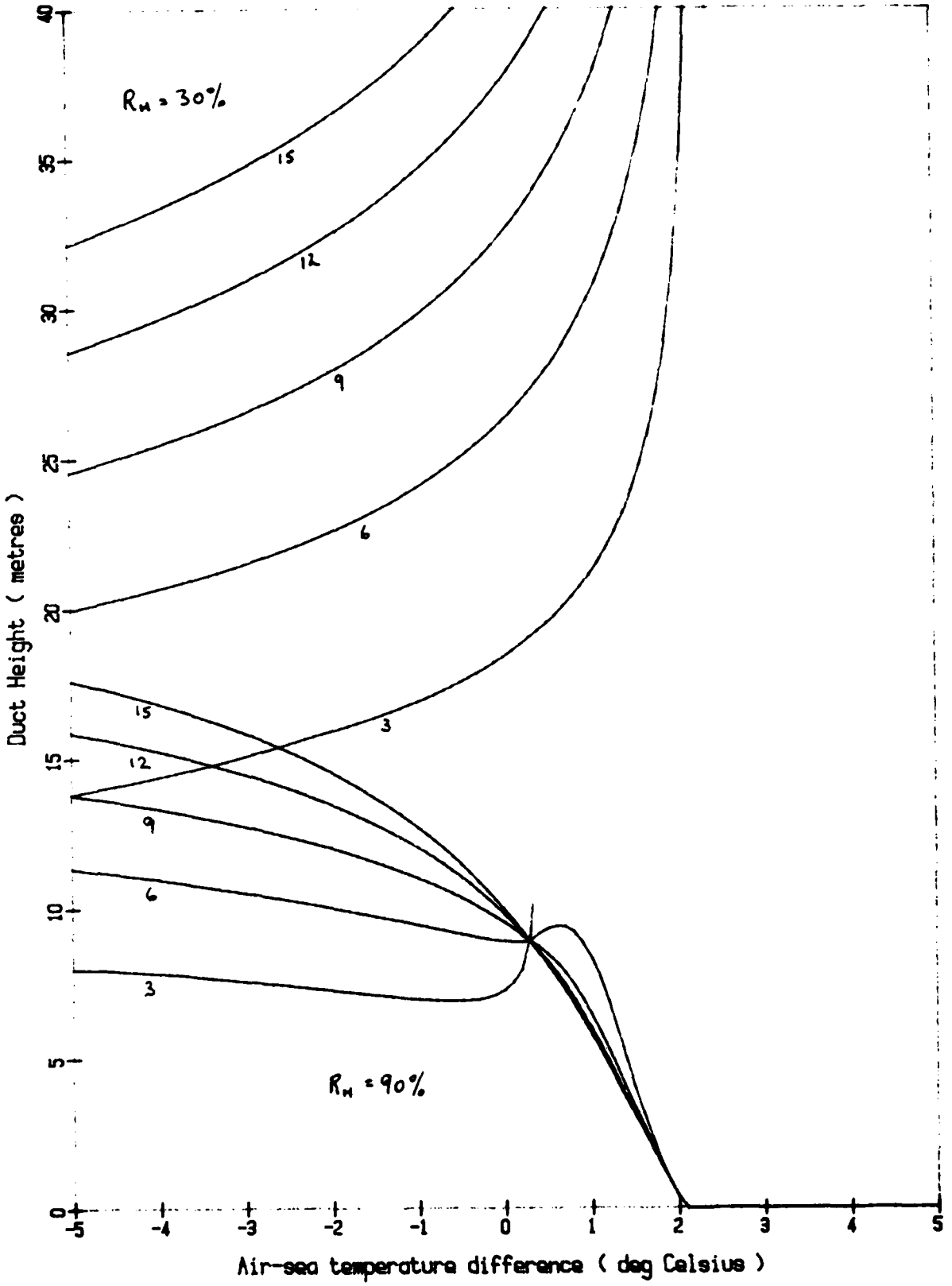

Figure 5. Calculated evaporative duct height for sea temperature of 24 deg C.
Wind speed : 3, 6, 9, 12, and 15 m/sec
Relative humidity : 30% and 90%
Measurement height : 10 metres

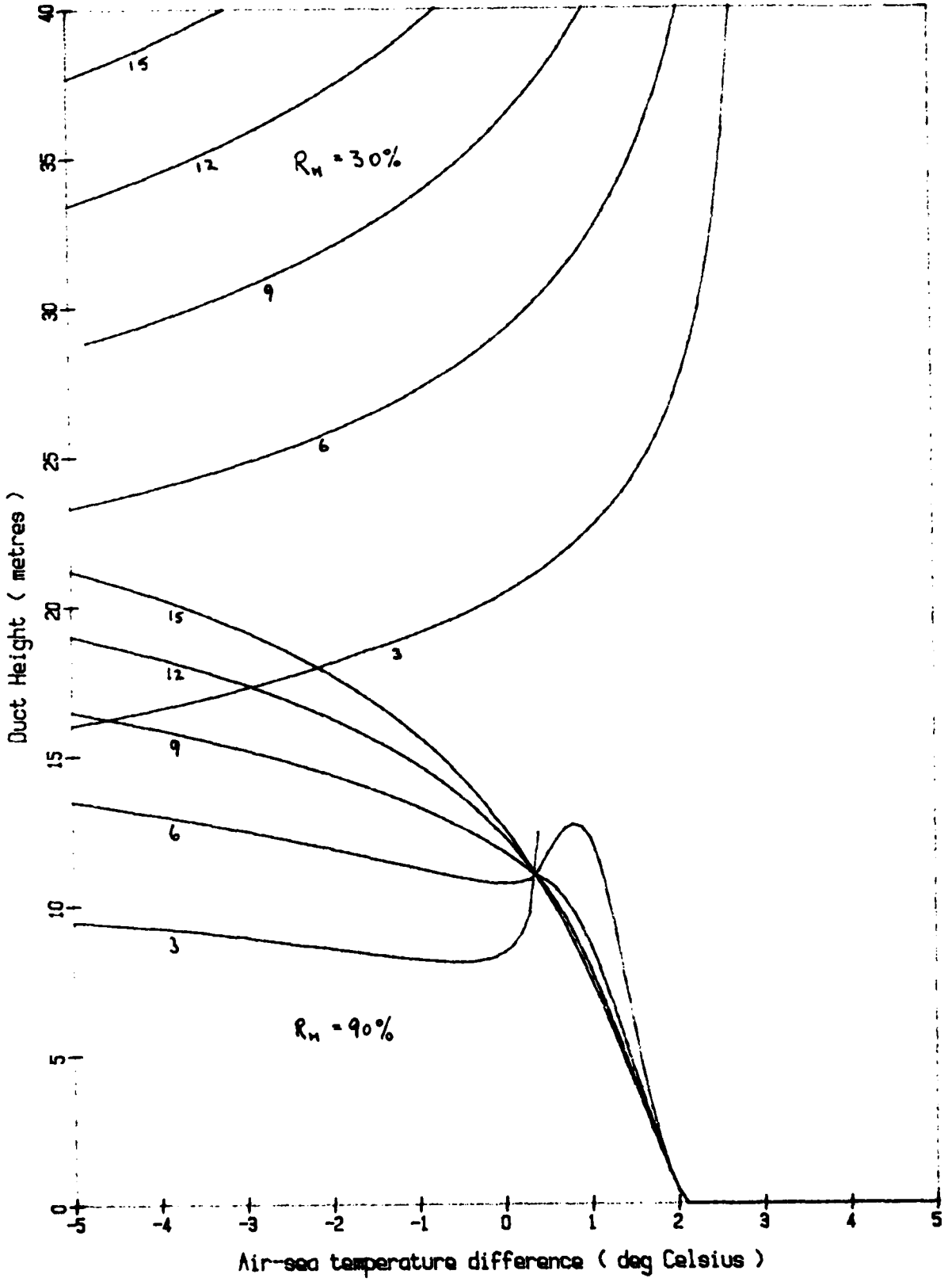

Figure 6. Calculated evaporative duct height for sea temperature of 28 deg C.
Wind speed : 3, 6, 9, 12, and 15 m/sec
Relative humidity : 30% and 90%
Measurement height : 10 metres

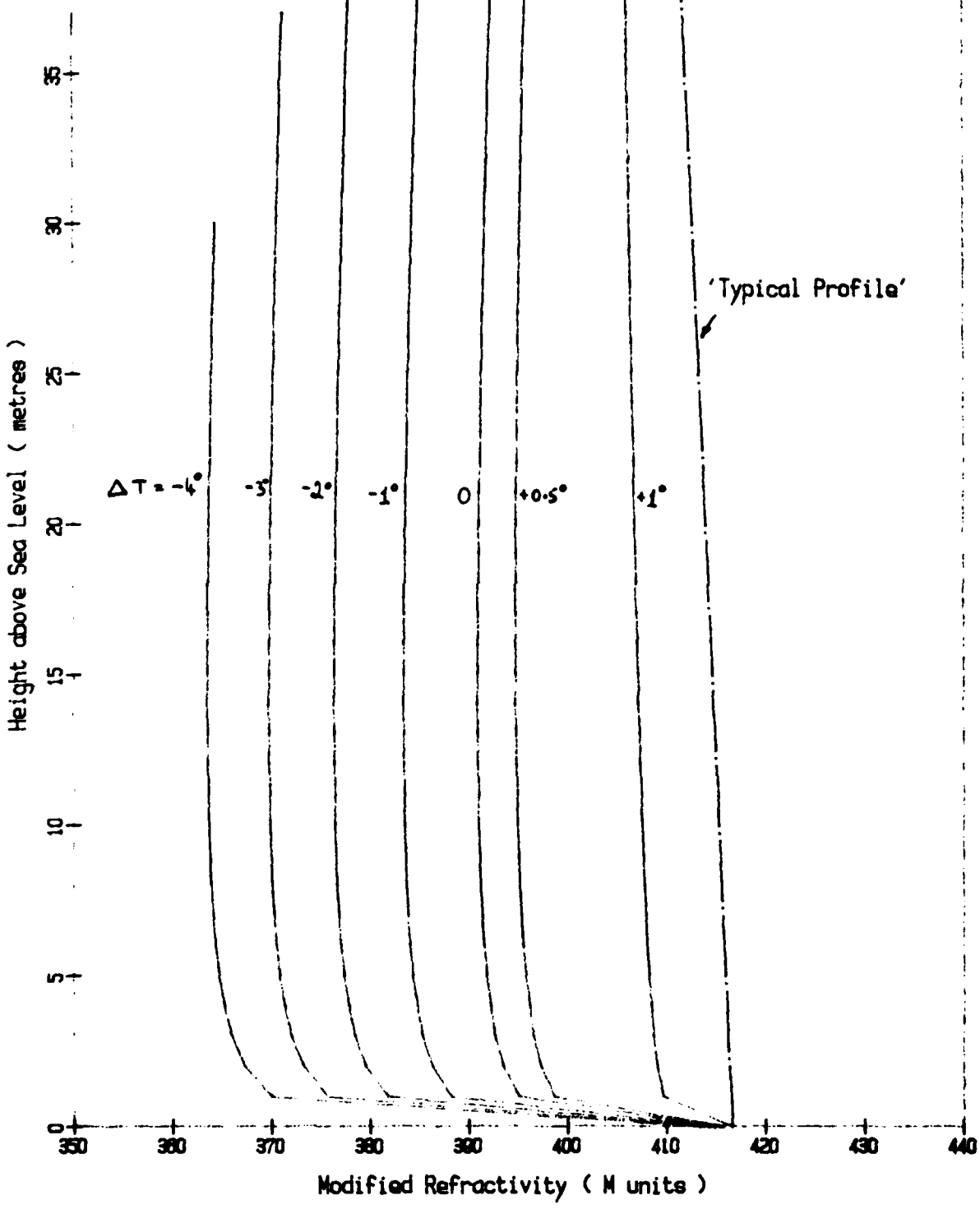

Figure 7. Modified refractivity for 7 air-sea temperature differences.
Sea temperature : 28 deg Celsius
Wind speed : 6 m/sec
Relative humidity : 85%
Measurement height : 10 metres

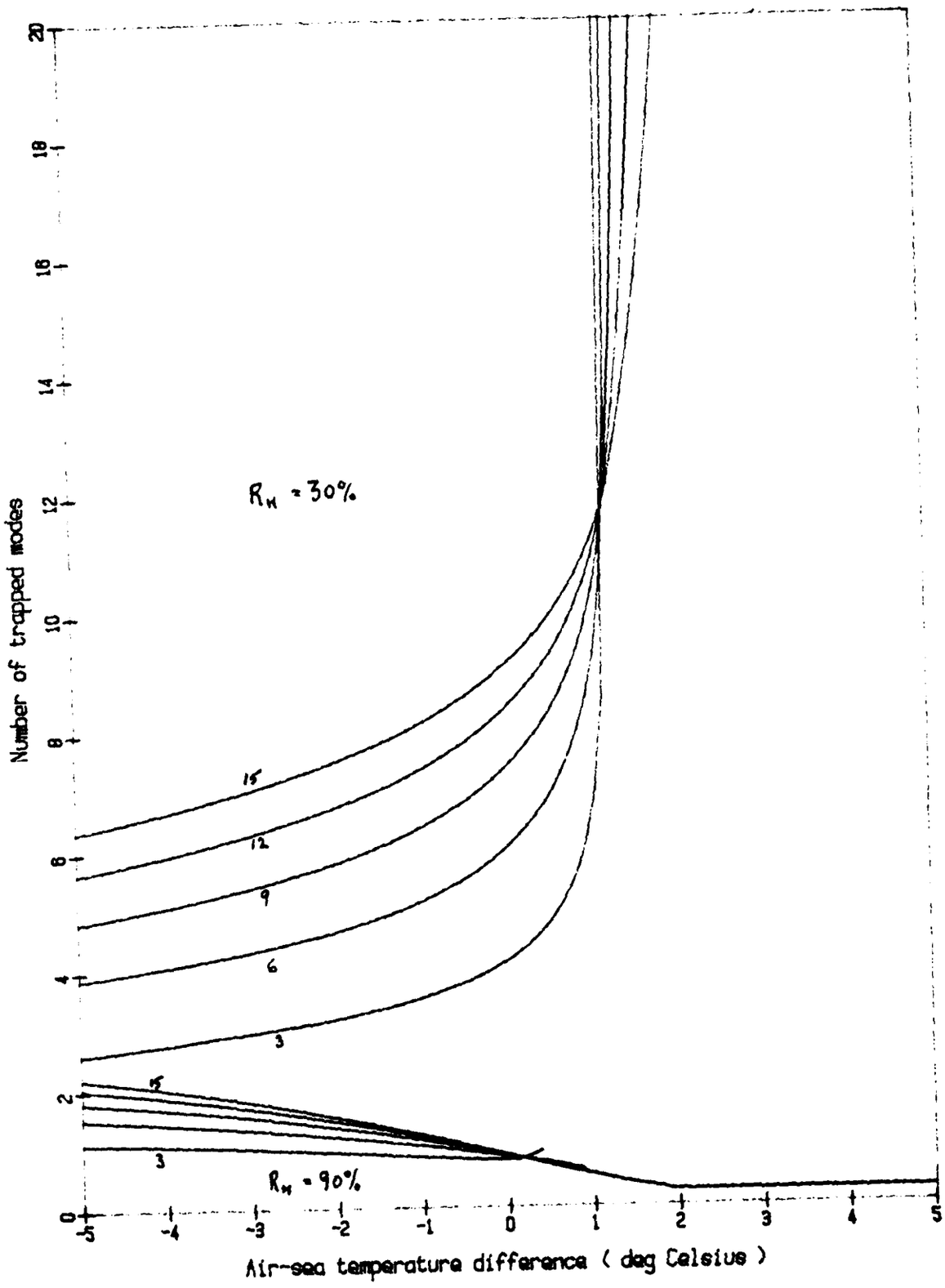

Figure 8. Number of trapped modes (m) at 10 GHz for sea temperature of 15 deg C.
Wind speed : 3, 6, 9, 12, and 15 m/sec
Relative humidity : 30% and 90%
Measurement height : 10 metres

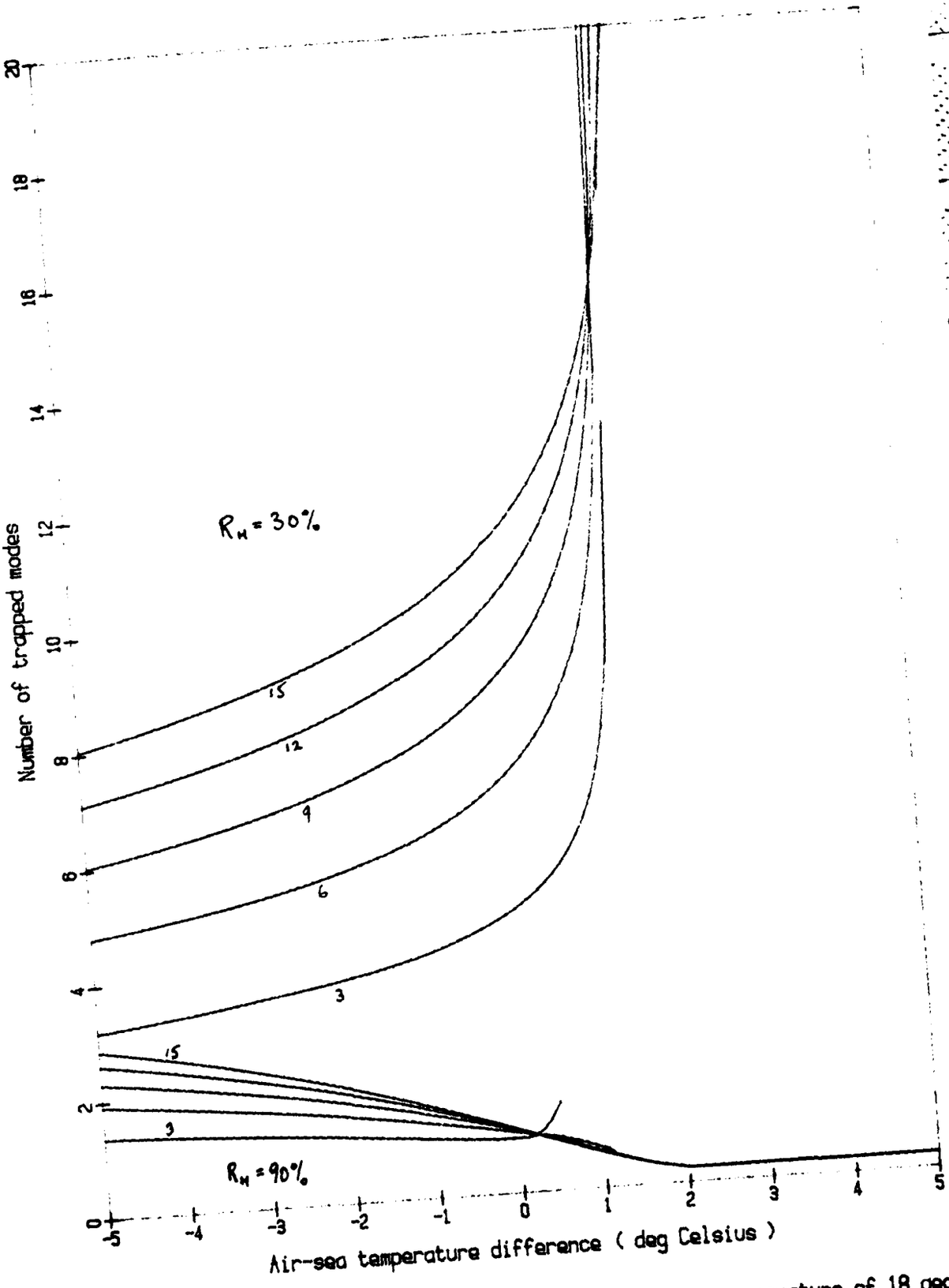

Figure 9. Number of trapped modes (m) at 10 GHz for sea temperature of 18 deg C.
Wind speed : 3, 6, 9, 12, and 15 m/sec
Relative humidity : 30% and 90%
Measurement height : 10 metres

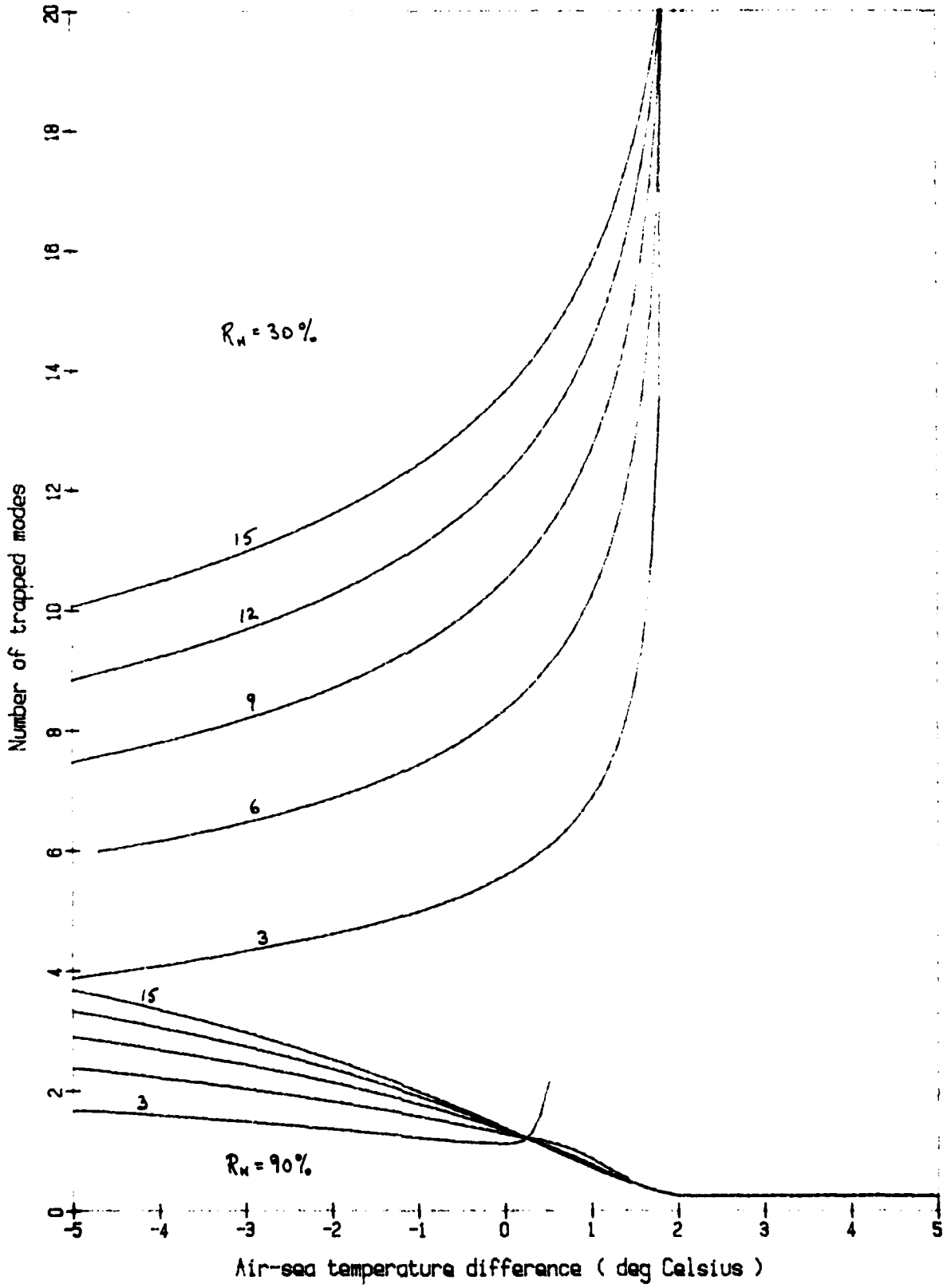

Figure 10. Number of trapped modes (m) at 10 GHz for sea temperature of 21 deg C.
Wind speed : 3, 6, 9, 12, and 15 m/sec
Relative humidity : 30% and 90%
Measurement height : 10 metres

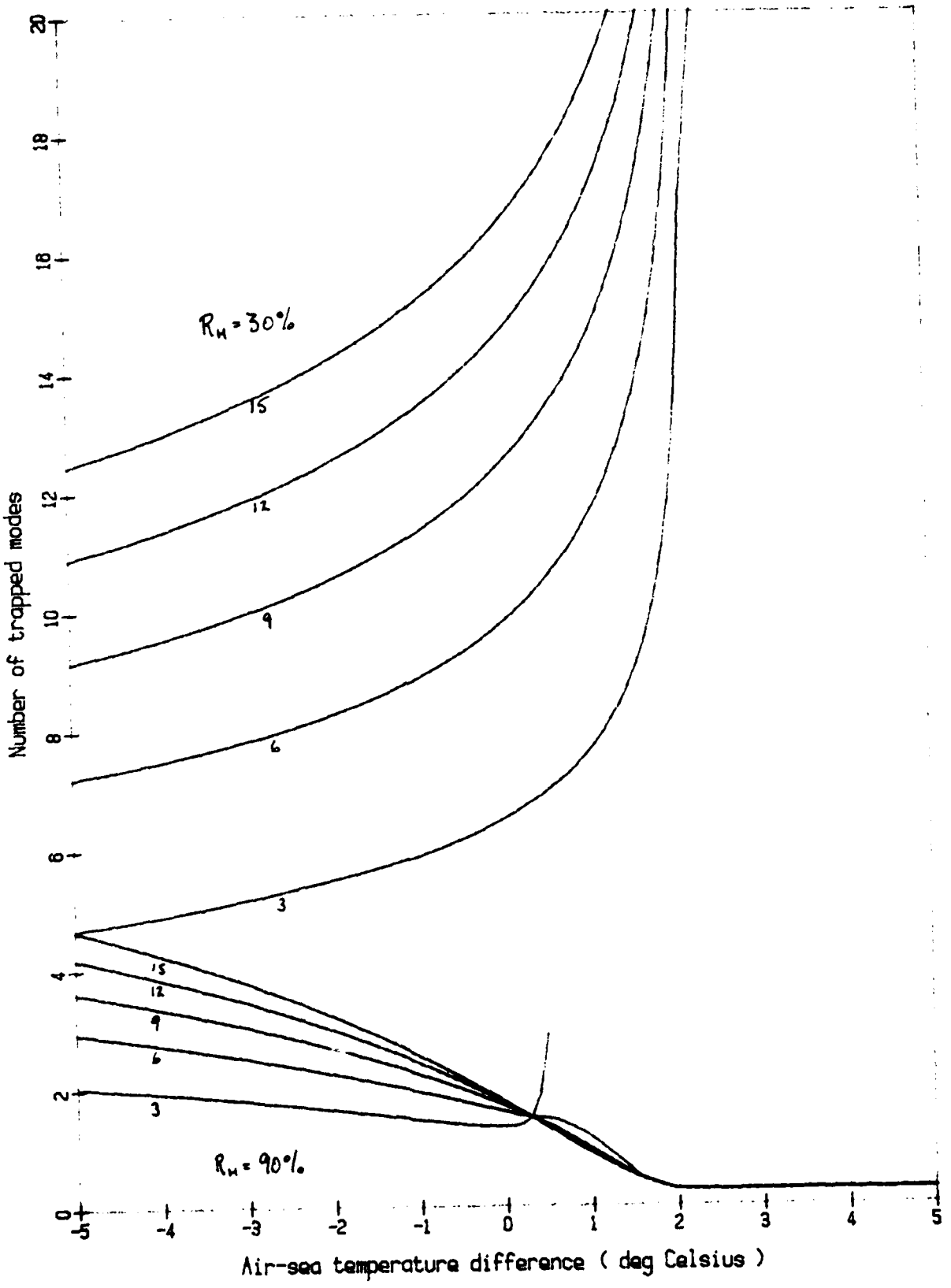

Figure 11. Number of trapped modes (m) at 10 GHz for sea temperature of 24 deg C.
Wind speed : 3, 6, 9, 12, and 15 m/sec
Relative humidity : 30% and 90%
Measurement height : 10 metres

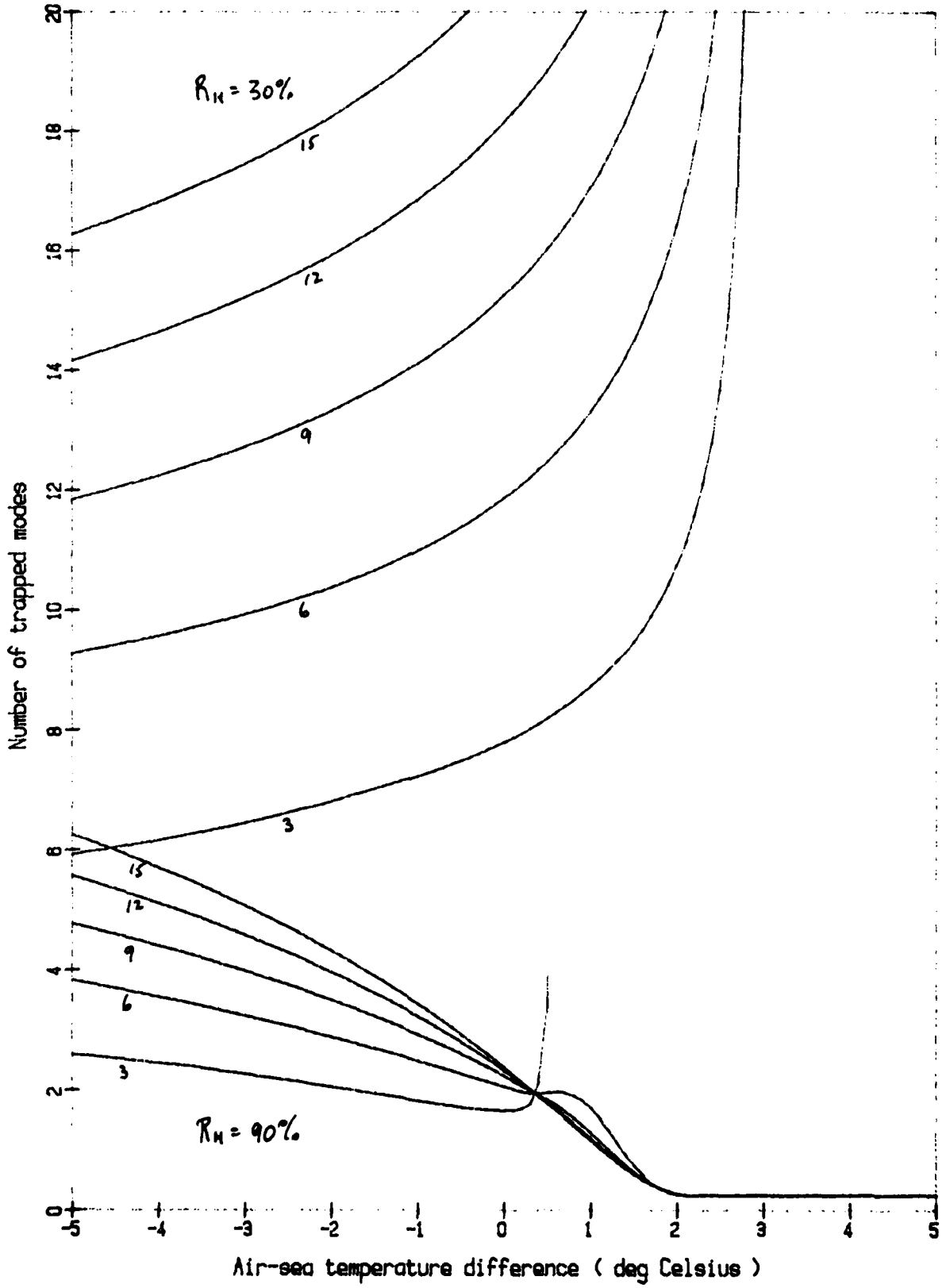

Figure 12. Number of trapped modes (m) at 10 GHz for sea temperature of 28 deg C.
Wind speed : 3, 6, 9, 12, and 15 m/sec
Relative humidity : 30% and 90%
Measurement height : 10 metres

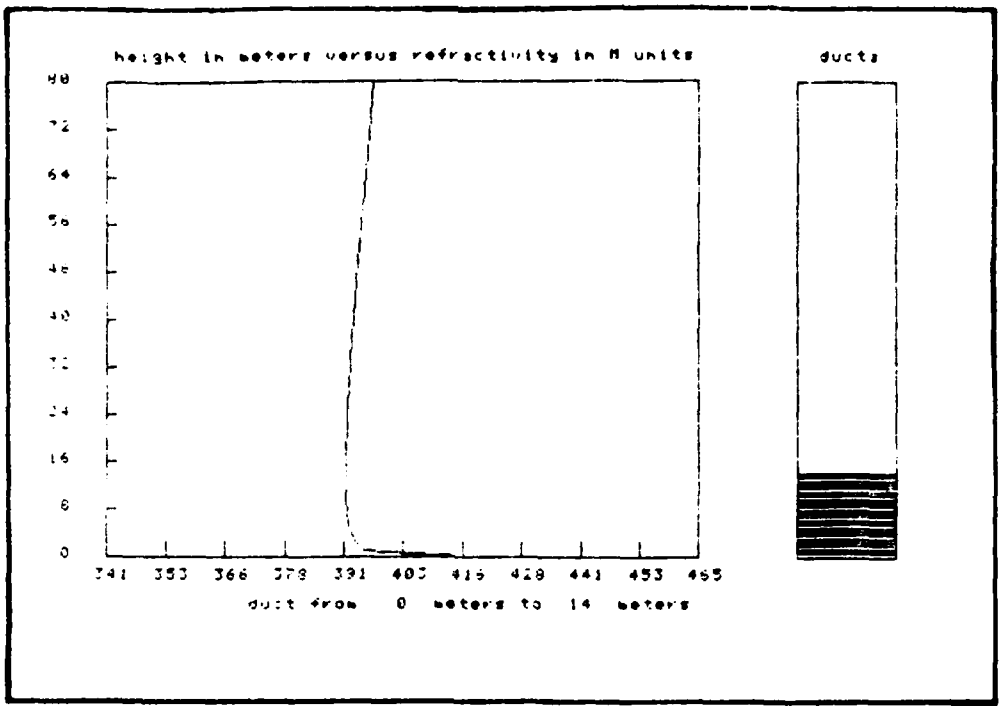

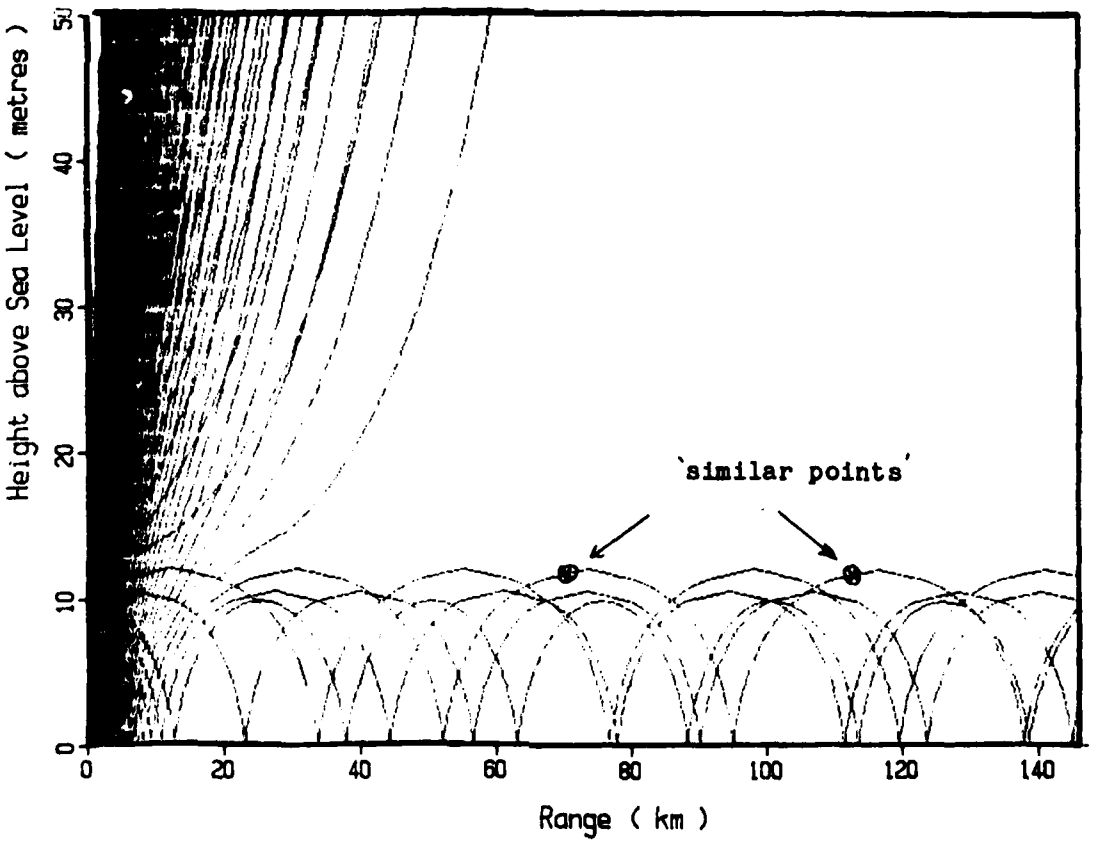

Figure 13. Ray trace and Refractivity Profile using model described in text.
Environmental : Sea temp : 28 deg Celsius.
Stability : Neutral.
Relative humidity : 85% at 10 metres.
Ray coverage : +/- 1 degree from 10 metre transmitter height.

DISTRIBUTION

	Copy No.
Chief Defence Scientist	1
Deputy Chief Defence Scientist	1
CERPAS	1
SSPA	1
JIO (DSTI)	2
RANRL Library Master Copy	3
Librarian Technical Reports Centre, Defence Central Library, Campbell Park.	4
OIC Document Exchange Centre DISB	5 - 22
Flag Officer Commanding HM Australian Fleet	23
Director General, Naval Operational Requirements	24
Director of Tactics, AIO and Navigation	25
Director of Operational Analysis - Navy	26
Director of Surface and Air Weapons - Navy	27
Director of Electronic Warfare - Navy	28
Director of Naval Oceanography and Meteorology	29
Director, RAN Tactical School	30
Director, Weapons Systems Research Laboratory	31
Director, Electronics Research Laboratory	32
Senior Librarian, Defence Research Centre Salisbury	33
Senior Librarian, Aeronautical Research Laboratories	34
Librarian H Block Victoria Barracks, Melbourne	35
Superintendent, Analytical Studies	36
Navy Scientific Adviser	37
Air Force Scientific Adviser	38
Director of Operational Analysis - Air Force	39
Dr P. Baker, Electronics Research Laboratory	40
Dr M.R. Battaglia	41
Dr I.S.F. Jones	42
RANRL Library	43 - 47
AGPS	48

Department of Defence

DOCUMENT CONTROL DATA

1. a. AR No	1. b. Establishment No	2. Document Date	3. Task No
003-429	RANRL-TN-3/85	April 1985	

4. Title	5. Security	6. No Pages
MODELLING THE RADAR EVAPORATIVE DUCT	a. document: UNCLAS b. title c. abstract: UNCLAS	43 7. No Refs: 19

8. Author(s)	9. Downgrading Instructions
BATTAGLIA, M.R.	N/A

10. Corporate Author and Address	11. Authority *(as appropriate)* a.Sponsor b.Security c.Downgrading d.Approval
RAN Research Laboratory PO Box 706 DARLINGHURST. NSW 2010	a. Operations Research Group b. HORG c. N/A(unclass) d. Dr. W. G. P. Robertson DWSRL

12. Secondary Distribution *(of this document)*

Approved for Public Release

Overseas enquirers outside stated limitations should be referred through ASDIS, Defence Information Services Branch, Department of Defence, Campbell Park, CANBERRA ACT 2601

13. a. This document may be ANNOUNCED in catalogues and awareness services available to ...

No limitations

13. b. Citation for other purposes *(ie casual announcement)* may be *(select)* unrestricted *(or)* as for 13 a.

14. Descriptors	15. COSATI Group
Radar, model, evaporative duct, micrometeorology	2004, 1709, 0401

16. Abstract

A model of the radar evaporative duct is described, based on Monin-Obukov similarity theory. The similarity functions, Monin-Obukov stability length and scaling parameters are derived from experimental data. Graphs are presented for duct heights and the number of trapped modes at 10 GHz for a wide range of experimental conditions.